Crystallization Behavior of $(Cu_{60}Zr_{30}Ti_{10})_{99}Sn_1$ Bulk Metallic Glass

Hao WANG[1)†], *Xiaoping SONG*[1,2)], *Xiangdong YAO*[1)], *Haifeng ZHANG*[2)] *and Zhuangqi HU*[2)]
1) Division of Materials, School of Engineering, The University of Queensland, Brisbane, QLD 4072, Australia
2) Institute of Metal Research, Chinese Academy of Sciences, Shenyang 110016, China
[Manuscript received January 24, 2005]

The crystallization behavior and crystallization kinetics of $(Cu_{60}Zr_{30}Ti_{10})_{99}Sn_1$ bulk metallic glass was studied by X-ray diffractometry and differential scanning calorimetry. It was found that a two-stage crystallization took place during continuous heating of the bulk metallic glass. Both the glass transition temperature T_g and the crystallization peak temperatures T_p displayed a strong dependence on the heating rate. The activation energy was determined by the Kissinger analysis method. In the first-stage of the crystallization, the transformation of the bulk metallic glass to the phase one occurred with an activation energy of 386 kJ/mol; in the second-stage, the formation of the phase two took place at an activation energy of 381 kJ/mol.

KEY WORDS: Bulk metallic glasses; Crystallization behavior; Cu-based BMG

1. Introduction

Cu-based bulk metallic glasses (BMG) have been produced in Cu-Ti-Zr-Ni[1], Cu-Ti-Zr-Ni-Si[2] and Cu-Ti-Zr-Ni-Sn[3] systems, however, the Cu content in these BMGs are all lower than 40 at. pct. In recent years, new bulk metallic glasses with a high Cu content of 60 at. pct were obtained in a ternary system Cu-(Zr or Hf)-Ti systems by Inoue group[4,5]. The alloys were based on the binary $Cu_{60}Zr(Hf)_{40}$ system. Ti addition at about 10 at. pct, which replaced Zr or Hf, significantly improved the glass-forming ability (GFA) of the binary alloy. Bulk metallic glasses with a diameter of 4 mm was reported in $Cu_{60}Zr_{30}Ti_{10}$. The material exhibited a high tensile strength exceed 2000 MPa, which was higher than the Zr-based BMGs. Due to their higher strength and lower cost, the new BMG materials have received great interest, and attempt has been made to further increase their critical diameter. Recently, it was found that the addition of Sn element can improve the GFA of the $Cu_{60}Zr_{30}Ti_{10}$ alloy[6]. A BMG rod of 5 mm diameter has been successful obtained in $(Cu_{60}Zr_{30}Ti_{10})_{99}Sn_1$ using Cu mould casting. In this paper, the glass transition and crystallization behavior of $(Cu_{60}Zr_{30}Ti_{10})_{99}Sn_1$ are studied

2. Experimental Procedures

Multicomponent alloy ingots with composition of $(Cu_{60}Zr_{30}Ti_{10})_{99}Sn_1$ was prepared by arc melting the mixtures of pure metals in a high purity Ar atmosphere purified using Ti getter. Cylindrical rods with a length of 50 mm and various diameters of 1∼6 mm were produced by Cu mould casting.

The structure of the samples was examined by X-ray diffractometry (XRD) with monochromatic Cu$K\alpha$ radiation. The glass transition and crystallization behavior of all samples were examined with a differential scanning calorimeter (Perkin-Elmer DSC7). The heating rates were 10, 15, 20, 30 and 40 K/min, respectively. The Kissinger analysis method was used to determine the activation energy for phase crystallization[7].

3. Results and Discussion

Formation of the metallic glass was examined by X-ray diffractometry. Figure 1 shows XRD patterns of as-cast rods of $(Cu_{60}Zr_{30}Ti_{10})_{99}Sn_1$ alloy. A broad diffraction characteristic of metallic glass is exhibited in the rod up to 5 mm in diameter. No diffraction peaks from crystalline phases are detected, indicating the formation of a single amorphous phase. For the sample with 6 mm in diameter, the XRD pattern shows sharp peaks from the crystalline phase superimposed on the broad halo peak, indicating the coexistence of crystalline and amorphous phases.

Figure 2 shows the DSC curve of $(Cu_{60}Zr_{30}Ti_{10})_{99}Sn_1$ at a heating rate of 20 K/min. The metallic glass exhibits a glass transition at 723 K, followed by a supercooled liquid region and then two well separated exothermic peaks at 765 and 810 K, respectively. The DSC curve of $Cu_{60}Zr_{30}Ti_{10}$ alloy was reported having the similar pattern with two separated exothermic peaks[8].

The as-cast samples were then annealed at different temperatures corresponding to the exothermic peaks observed in the DSC curve. Figure 3 shows the XRD patterns of $(Cu_{60}Zr_{30}Ti_{10})_{99}Sn_1$ alloy after isothermal annealing at 730 K (after glass transition but before crystallization), 760 K (after the onset of the first exothermic reaction), 800 K (after the onset of the second exothermic reaction) and 900 K (after completion of all crystallization) for 10 min. The sample annealed at the temperature just after glass transition shows a broad peak corresponding to the amorphous phase. Some crystalline peaks are super-

† Ph.D., to whom correspondence should be addressed,
E-mail: H.Wang@minmet.uq.edu.au.

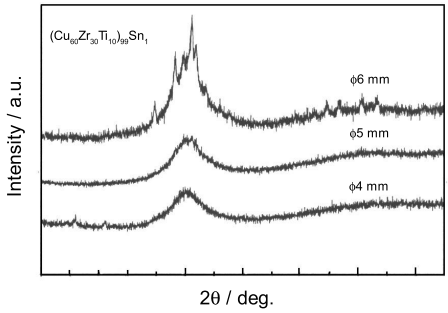

Fig.1 XRD patterns of the as-cast $(Cu_{60}Zr_{30}Ti_{10})_{99}Sn_1$ rods with diameters of 4, 5 and 6 mm

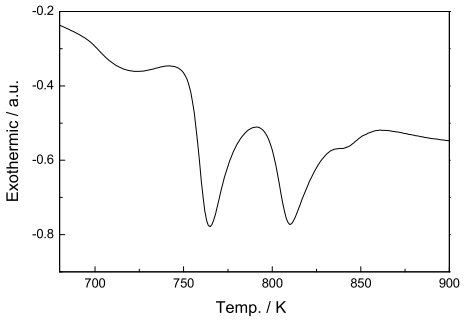

Fig.2 DSC curve of the as-cast rod of $(Cu_{60}Zr_{30}Ti_{10})_{99}Sn_1$ at a heating rate of 20 K/min

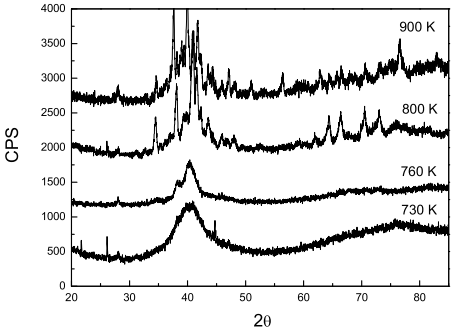

Fig.3 XRD patterns of $(Cu_{60}Zr_{30}Ti_{10})_{99}Sn_1$ annealed at 730, 760, 800 and 900 K for 10 min

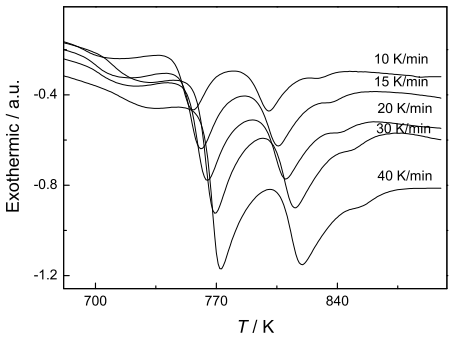

Fig.4 DSC curves of $(Cu_{60}Zr_{30}Ti_{10})_{99}Sn_1$ alloy at different heating rates

imposed on the broad peak. After the first exothermic reaction (annealed at 760 K), the XRD pattern shows the initial crystallization. The broad amorphous peak is split into two. Louzguine described the crystallization products for $Cu_{60}Zr_{30}Ti_{10}$ at this stage as phase 1, which was found to have cubic symmetry[8]. After the exothermic reaction 2, significant crystallization occurred. The broad peak is replaced by sharp peaks from crystalline phases. The crystalline phases are indexed as the Cu_8Zr_3 and Cu_3Ti_2 and some unknown phases, which are similar to that in $Cu_{60}Zr_{30}Ti_{10}$ alloy. Louzguine described the crystallization products for this stage as phase 2[8]. 900 K annealing should result in the equilibrium crystallization products. XRD pattern indicates that some different phases are also precipitated.

DSC traces taken at different heating rates were used to determine activation energy for the crystallization. Figure 4 shows the continuous heating DSC curves of $(Cu_{60}Zr_{30}Ti_{10})_{99}Sn_1$ alloy at heating rates of 10, 15, 20, 30 and 40 K/min, respectively. The glass transition temperature T_g, the onset temperatures for the exothermic reactions T_{x1} and T_{x2}, and the peak temperatures T_{p1} and T_{p2} for different heating rate are listed in Table 1. It can be seen all these temperatures are shifted to higher temperatures with the increase of heating rate. Both the crystallization temperature and glass transition temperature display a dependence on the heating rate during continuous heating. This phenomenon indicates that the glass transition and the crystallization of the BMG alloy behaves in a marked kinetic nature.

The Kissinger analysis method was used to determine the kinetic constants of phase transformations observed in DSC[7]. In this method, Eq.(1) describes the fraction transformed as a function of time and temperature:

$$\frac{\mathrm{d}x}{\mathrm{d}t} = A(1-x)\exp\left(\frac{-E}{RT}\right) \tag{1}$$

where E is the activation energy for crystallization, x is fraction transformed, t is time. The E value can be obtained directly from the temperature T_p (peak temperature) at which the derivative $\mathrm{d}x/\mathrm{d}t$, the transformation rate, attains its maximum value. Solving Eq.(1) for $(\mathrm{d}/\mathrm{d}t)$ $(\mathrm{d}x/\mathrm{d}t)$ Kissinger derived the following formula:

$$-\frac{E}{R} = \mathrm{d}\left(\ln\frac{\beta}{T_p^2}\right)/\mathrm{d}\left(\frac{1}{T_p}\right) \tag{2}$$

where β is the heating rate $\mathrm{d}T/\mathrm{d}t$. As E is time- and temperature-independent, the plot $\ln(\beta/T_p^2)$ *vs* $1/T_p$ has a linear shape, which allows E to be calculated using the slope of the linear fit. This method has been applied to a large number of amorphous alloy and linearity of the $\ln(\beta/T_p^2)$ *vs* $1/T_p$ plot is well established[8,9].

The plots of $\ln(\beta/T_p^2)$ *vs* $1/T_p$ for the $(Cu_{60}Zr_{30}Ti_{10})_{99}Sn_1$ bulk metallic glass are shown in Fig.5. The plots also have a linear shape. The activation energy for the first crystallization stage is 386 kJ/mol and that for the second stage is 381 kJ/mol. Louzguine has reported that for $Cu_{60}Zr_{30}Ti_{10}$ the activation energy for crystallization is 265 kJ/mol[8]. The higher values of the activation energies in $(Cu_{60}Zr_{30}Ti_{10})_{99}Sn_1$ bulk metallic glass

Table 1 Glass transition temperature T_g, onset temperatures for the crystallization T_x, peak temperatures for the exothermic reactions T_{p1} and T_{p2} and supercooled liquid region $\Delta T(\Delta T = T_x - T_g)$ for $(Cu_{60}Zr_{30}Ti_{10})_{99}Sn_1$ alloy at different heating rates β

β/(K/min)	T_g/K	T_x/K	ΔT/K	T_{p1}/K	T_{p2}/K	$\ln\frac{\beta}{T_{p1}^2}$	$\frac{1}{T_{p1}} \times 10^{-3}$	$\ln\frac{\beta}{T_{p2}^2}$	$\frac{1}{T_{p2}} \times 10^{-3}$
10	714	736	22	756	800	−15.048	1.323	−15.161	1.250
15	721	741	20	761	805	−14.656	1.314	−14.768	1.242
20	723	742	19	765	810	−14.378	1.307	−14.493	1.235
30	732	745	13	769	815	−13.983	1.300	−14.100	1.227
40	735	748	13	773	819	−13.706	1.294	−13.822	1.221

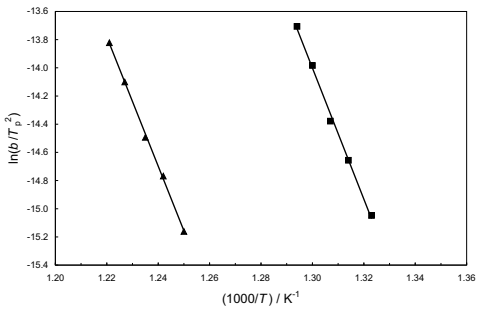

Fig.5 Kissinger plots of exothermic reactions for $(Cu_{60}Zr_{30}Ti_{10})_{99}Sn_1$

compared reflect its higher thermal stability and glass forming ability than $Cu_{60}Zr_{30}Ti_{10}$ alloy. It can be concluded that the increase of the critical size for BMG $(Cu_{60}Zr_{30}Ti_{10})_{99}Sn_1$ after the addition of Sn is the result of the increased activation energy for crystallization. It is expected the thermal stability will also improved.

4. Summary

The crystallization behavior and crystallization kinetics of $(Cu_{60}Zr_{30}Ti_{10})_{99}Sn_1$ bulk metallic glass was studied by X-ray diffractometry and differential scanning calorimetry. It was found that a two-stage crystallization took place during continuous heating of the bulk metallic glass. Both the glass transition temperature T_g and the crystallization peak temperatures T_p displayed a strong dependence on the heating rate. The activation energy for the two crystallization stages was 386 kJ/mol and 381 kJ/mol, which were higher than that from $Cu_{60}Zr_{30}Ti_{10}$. Addition of Sn increased the activation energy for crystallization, therefore the glass-forming ability and thermal stability for the BMG alloy were improved.

Acknowledgements

The work is financially supported by the Australia Research Council through an International Linkage project. The authors would like to thank Dr Q.S. Zhang from the Institute of Metals Research, China for providing the BMG samples, Dr T. Sercombe from the University of Queensland for his assistance on DSC experiment and Dr D.V. Louzguine from Tohoku University for useful discussion.

REFERENCES

[1] X.H.Lin and W.L.Johnson: *J. Appl. Phys.*, 1995, **78,** 6514.
[2] T.Zhang and A.Inoue: *Mater. Trans. JIM*, 1999, **40,** 301.
[3] C.Li, J.Saida, M.Kiminami and A.Inoue: *J. Non-Cryst. Solids*, 2000, **261,** 108.
[4] A.Inoue, W.Zhang, T.Zhang and K.Kurosaka: *Mater. Trans.*, 2001, **42,** 1149.
[5] A.Inoue, W.Zhang, T.Zhang and K.Kurosaka: *Acta Mater.*, 2001, **49,** 2645.
[6] Q.S.Zhang, H.F.Zhang, Y.F.Deng, B.Z.Ding and Z.Q.Hu: *Scripta Mater.*, 2003, **49,** 273.
[7] H.E.Kissinger: *J. Res. National Bureau Stand.*, 1956, **57,** 217.
[8] D.V.Louzguine and A.Inoue: *J. Mater. Res.*, 2002, **17,** 2112.
[9] D.V.Louzguine and A.Inoue: *Appl. Phys. Lett.*, 2002, **81,** 2561.